



Abrupt onset and termination of the African Humid Period: rapid climate responses to gradual insolation forcing

Peter deMenocal^{a,*}, Joseph Ortiz^a, Tom Guilderson^b, Jess Adkins^a, Michael Sarnthein^c,
Linda Baker^a, Martha Yarusinsky^a

^aLamont-Doherty Earth Observatory of Columbia University, Palisades, NY 10964, USA

^bCenter for Accelerator Mass Spectrometry, Lawrence-Livermore National Laboratory, Livermore CA 94551, USA

^cInstitute fuer Geowissens Chafter, Universitaet Kiel, Kiel, Germany

Abstract

A detailed (ca. 100 yr resolution) and well-dated (18 AMS ¹⁴C dates to 23 cal. ka BP) record of latest Pleistocene–Holocene variations in terrigenous (eolian) sediment deposition at ODP Site 658C off Cap Blanc, Mauritania documents very abrupt, large-scale changes in subtropical North African climate. The terrigenous record exhibits a well-defined period of low influx between 14.8 and 5.5 cal. ka BP associated with the African Humid Period, when the Sahara was nearly completely vegetated and supported numerous perennial lakes; an arid interval corresponding to the Younger Dryas Chronozone punctuates this humid period. The African Humid Period has been attributed to a strengthening of the African monsoon due to gradual orbital increases in summer season insolation. However, the onset and termination of this humid period were very abrupt, occurring within decades to centuries. Both transitions occurred when summer season insolation crossed a nearly identical threshold value, which was 4.2% greater than present. These abrupt climate responses to gradual insolation forcing require strongly non-linear feedback processes, and current coupled climate model studies invoke vegetation and ocean temperature feedbacks as candidate mechanisms for the non-linear climate sensitivity. The African monsoon climate system is thus a low-latitude corollary to the bi-stable behavior of high-latitude deep ocean thermohaline circulation, which is similarly capable of rapid and large-amplitude climate transitions. © 1999 Elsevier Science Ltd. All rights reserved.

1. Introduction

During the latest Pleistocene and early Holocene, the now hyperarid Saharan desert was a verdant landscape nearly completely vegetated with annual grasses and shrubs (COHMAP Members, 1988; Jolly, 1998; Sarnthein, 1978). At that time, subtropical North Africa was characterized by numerous large and small lakes which supported abundant savannah and lake margin fauna such as antelope, giraffe, elephant, hippopotamus, crocodile, and human populations in regions that today have almost no measurable precipitation (McIntosh and McIntosh, 1983). The Holocene African Humid Period occurred between ca. 9 and 6 cal. ka BP (Ritchie et al., 1985; Roberts, 1998), but humid conditions had initially commenced by ca. 14.5 cal. ka BP following full glacial

hyperarid conditions during the latest Pleistocene (COHMAP Members, 1988; Street and Grove, 1979; Street-Perrot, et al., 1990; Sarnthein et al., 1982).

The early Holocene greening of North Africa has been linked to an intensification of the African monsoon due to earth orbital changes which increased summer season insolation forcing of the African monsoon. By 10–11 cal. ka BP, summer insolation in the Northern Hemisphere had risen to peak levels approximately 8% greater than today due to earth's orbital precession which gradually aligned the boreal summer solstice with perihelion (Berger and Loutre, 1991). Monsoonal climate is effectively a thermodynamic heat engine response to seasonal radiation forcing (Webster, 1987). During boreal summer, the North African land surface is heated more efficiently than the adjacent oceans and this establishes a strong low pressure center over North Africa. It is this land–sea pressure gradient which largely drives the strong cyclonic inflow of moist maritime surface winds and brings the heavy and highly seasonal monsoonal precipitation during the boreal summer months.

* Corresponding author. Tel.: 001-914-365-8483; fax: 001-914-365-8165. Lamont-Doherty Earth Observatory, of Columbia University, Geoscience 211, Palisades, NY 10964, USA.

E-mail address: peter@ldeo.columbia.edu (P. deMenocal)

Climate modeling studies have abundantly documented the strong sensitivity of monsoonal climate to orbital changes in summer season insolation (deMenocal and Rind, 1993; Kutzbach and Guetter, 1986; Kutzbach and Otto-Bliesner, 1982; Pokras and Mix, 1987; Prell and Kutzbach, 1987). Orbital variations cause changes in the seasonal distribution of incident solar radiation, and resulting changes in summer season insolation affect the strength of the summer monsoon. Using an atmosphere-only climate model, Prell and Kutzbach (1987) found that precipitation over North Africa increased by a factor of five over the proportional increase in summer radiation. For example, North African rainfall increased by approximately 40% (relative to the control experiment) resulting from the 8% increase in summer radiation forcing. These orbital variations in monsoonal surface wind and precipitation fields affected not only African terrestrial climate, but also the surface circulation of adjacent tropical and subtropical which are dynamically linked to the associated monsoonal surface wind field perturbations (Anderson and Prell, 1992; Clemens et al., 1991; Clemens and Prell, 1990; McIntyre et al., 1989; Molino and McIntyre, 1990b; Rossignol-Strick, 1985; Tiedemann et al., 1994).

Despite the very high sensitivity of African monsoonal precipitation to orbital insolation forcing in atmosphere-only models, the calculated increases in the surface hydrological budget were apparently insufficient to have established large standing lakes in simulations of the early Holocene (Broström et al., 1998; Coe and Bonan, 1997; Kutzbach, 1996). It is only when coupled ocean model and responsive land surface (vegetation) model elements are incorporated into the simulations that Africa can become sufficiently humid year-round to support numerous large perennial lakes in the Sahara as the geologic data document, such as Lake MegaChad which spanned 330,000 km² (Broström et al., 1998; Coe and Bonan, 1997; Kutzbach, 1996). Parallel early Holocene increases in surface ocean temperature, vegetation cover (lower albedo), and moisture availability are positive feedback amplifications which locally match or exceed radiative effects due the initial insolation forcing alone (Broström et al., 1998; Coe and Bonan, 1997; Foley et al., 1994; Hoelzmann et al., 1998; Kutzbach, 1996; Kutzbach & Liu, 1997; Masson and Joussaume, 1997; Kohfeld and Harrison, 1999 this issue). Land surface climate and coupled ocean–atmosphere responses to boundary condition changes are notoriously non-linear. In these more complex model simulations, gradual boundary condition forcing such as orbital insolation change commonly results in a rectified integrated climate response which is rapid and abrupt (Claussen et al., 1998; Manabe and Stouffer, 1995; Rahmstorf, 1995).

How abrupt were the climate shifts associated with the onset and termination of the African Humid Period? Geologic evidence documenting the mid-Holocene ter-

mination of the African Humid Period suggests a relatively abrupt shift toward more arid conditions which occurred between ca. 5 and 6 cal. ka BP associated with the gradual decline in summer season radiation (Gasse and Van Campo, 1994; Petit-Maire and Guo, 1996; Street and Grove, 1979; Street-Perrott and Harrison, 1984). Lake levels fell sharply (Street and Grove, 1979), fossil pollen records from African lake basins show a rapid retreat of mesic taxa (Lamb et al., 1995; Lezine, 1991; Lezine et al., 1990; Sarnthein et al., 1982) and sedentary, lacustrine-tradition human populations in the central and southern Sahara were rapidly replaced by mobile, pastoralist-tradition cultures (McIntosh and McIntosh, 1983). Terrestrial geologic records of the African Humid Period are commonly incomplete due to subsequent desiccation and erosion of paleolake basin sequences, which furthermore can be difficult to date due to local hard water reservoir effects. With a few notable exceptions, marine sediment sequences commonly lack the temporal resolution needed to define century-scale climatic shifts. Our strategy here is to reconstruct a detailed marine sediment record of the export of windborne African dust and document its variability over the last 25 cal. ka BP.

2. Site location and climatic setting

We present a continuous, well-dated, and high-resolution (50–100 yr sampling) marine sediment record of Late Pleistocene–Holocene changes in West African climate which records both the timing and abruptness of the onset and termination of the African Humid Period. Ocean Drilling Program Site 658C was cored off Cap Blanc, Mauritania (20°45'N, 18°35'W, 2263m; Ruddiman et al., 1988) during ODP Leg 108. This core has a high accumulation rate (18 cm/kyr average) due to the dual influences of high regional surface ocean productivity and high supply of windblown Africa dust (Fig. 1) (Sarnthein and Tiedemann, 1989). Northeast Trade winds parallel the Northwest African margin and resulting surface water divergence promotes upwelling of cold, nutrient-rich waters which support high surface productivity and high biogenic particle fluxes to the seafloor throughout the year (Fischer et al., 1996).

Site 658C is ideally situated to monitor past variations in northwest African climate. The site is positioned directly below the axis of the summer African dust plume which transports an estimated 400×10^6 tons of mineral aerosol dust annually from the sub-Saharan and Sahel regions of Northwest Africa to the adjacent eastern subtropical Atlantic (Fig. 1) (Tetslaff and Wolter, 1980; Pye, 1987). Mineralogic and geochemical data document the dominant influence of these windborne African dusts on the composition of marine sediments in the eastern subtropical Atlantic, particularly along the Northwest

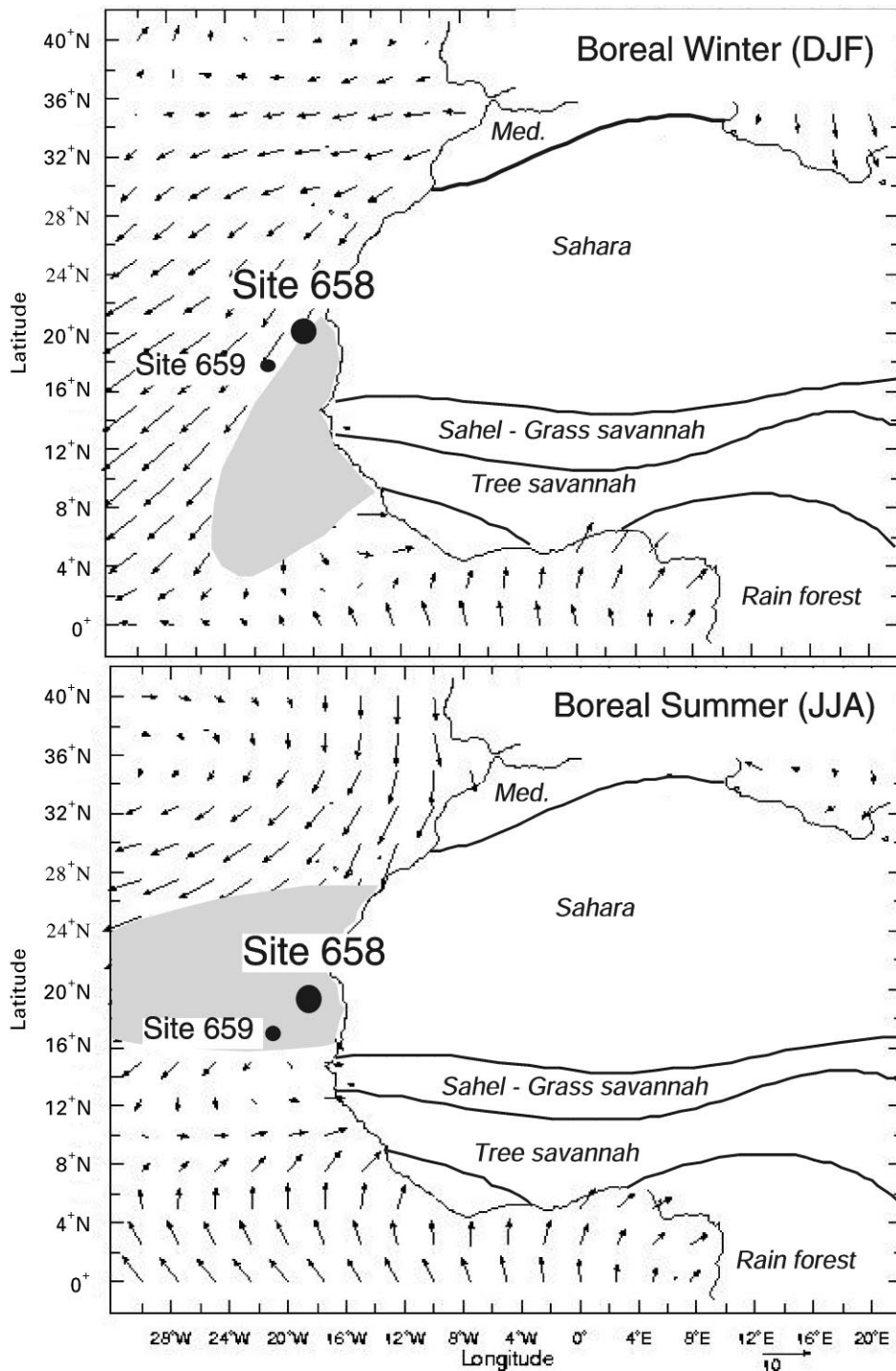


Fig. 1. Seasonal climatology of surface winds, rainfall, and atmospheric dust trajectories over subtropical West Africa. During boreal winter months the land surface cools relative to the ocean and regional atmospheric circulation is dominated by the NE trade winds which advect African dust to the eastern equatorial Atlantic. The winter African dust trajectory (stippled pattern) follows the NE-SW pattern of the transporting winter trade winds (Pye, 1987). During boreal summer increased sensible heating over central North Africa drives the cyclonic inflow of moisture-laden air from the adjacent eastern equatorial Atlantic which brings sporadic but intense monsoon rains to the sub-Saharan and Sahel regions of West Africa. The summer African dust plume (stippled pattern) results from strong surface turbulence associated with monsoonal frontal systems and entrained particles are convectively lifted to mid-tropospheric levels and then transported westward by the African Easterly Jet (Pye, 1987; Schütz et al., 1981). Interannual variations in African dust export are highly correlated to regional precipitation anomalies (Prospero, 1981; Prospero and Nees, 1977; Prospero and Nees, 1986). The location of Ocean Drilling Program Site 658 off Cap Blanc, Mauritania is shown.

African margin between 20 and 30°N (Sarnthein et al., 1982; Grousset et al., 1998; Kolla et al., 1979). During boreal summer, frontal systems associated with the easterly-propagating jet generate strongly turbulent surface winds which entrain mineral aerosols from immature soils and desert sands (Pye, 1987). The combination of turbulent suspension and vertical convection lifts aerosol-laden airmasses to the middle troposphere which are then entrained into the African Easterly Jet and carried westward (Fig. 1). African dust crosses the Atlantic in roughly six days. In the vicinity of Site 658, the wind-borne terrigenous sediment is composed of fine silt-sized subrounded quartz and feldspar grains with an associated illitic matrix reflecting the highly weathered dust source areas of the African desert (Grousset et al., 1998; Schütz et al., 1981).

Interannual increases in the export of African mineral aerosols to the subtropical Atlantic marine boundary layer are closely linked to negative annual precipitation anomalies in the dust source areas of West Africa (Middleton, 1987; Moulin et al., 1997; Prospero and Nees, 1977). A continuously monitored atmospheric aerosol sampling station in Barbados has been measuring year-to-year variations in African dust loading for many decades, and these data have documented greatly increased aerosol dust loading associated with drought conditions in Northwest Africa (Prospero and Nees, 1986). These drought periods reflect reductions in the strength and duration of the summer African monsoon which is the dominant source of annual precipitation to the region. Interannual variations in West African precipitation and atmospheric dust loading are evidently linked to persistent sea-surface temperature anomalies in the North Atlantic and tropical Atlantic sectors (Henning and Flohn, 1981; Druyan, 1987; Fontaine and Bigot, 1993; Moulin et al., 1997).

3. Analytical methods and age control

Core 1H from Site 658C was continuously subsampled at 2 cm intervals using a polycarbonate spatula; the sample interval is equivalent to between 50 and 150 yr depending on the interval sedimentation rate. The 658C depth scale used in this study was based on the cumulative section lengths which were recorded by ODP when Core 1H was first split for analysis (Core 1H: Section 1 (153 cm), Section 2 (154 cm), and Section 3 (155 cm)). We adopted this depth scale so that all analyses could be positioned subsequently and unequivocally within the context of the original archived sediments.

Samples were freeze-dried, weighed and a small portion of each sample was powdered and measured for carbonate and biogenic opal concentrations. Calcium carbonate was measured in all samples ($n = 227$) by coulometry to within 0.3% absolute by weight, and bio-

genic opal was measured in every other sample using the wet reduction spectrophotometric technique (Mortlock and Froelich, 1989) which had an absolute precision of 0.48% by weight for these sediments. Organic carbon was not measured for all samples but ranged between 0.5 and 1.5% in these samples. The residual terrigenous (detrital) sediment fraction was determined by first interpolating the opal data to obtain opal percent values for all samples, and residual terrigenous percentages were calculated by differencing. Average carbonate, opal, and terrigenous percentages at Site 658C were 42, 5, 53%, respectively (Fig. 2). Sediment wet bulk density was measured shipboard using the gamma-ray attenuation porosity evaluator (GRAPE), and these data were converted to dry bulk density using the shipboard physical property data for Site 658 (Ruddiman et al., 1988).

A benthic oxygen isotope stratigraphy was established by analyzing between 5 and 8 picked individuals of *Cibicides wuellerstorfi* from the washed $> 150 \mu\text{m}$ fraction of each sample. All samples were first sonicated in dionized water then analyzed on the Wood Hole Oceanographic Institution Finnigan MAT252 mass spectrometer with the Kiel automated carbonate preparation device. Samples were not roasted prior to analysis. The external precision of the isotopic analyses was $\pm 0.03\text{‰}$ for $\delta^{13}\text{C}$ and $\pm 0.07\text{‰}$ for $\delta^{18}\text{O}$ based on more than 1200 measurements of NBS19 standard.

Age control was established by accelerator mass spectrometry (AMS) radiocarbon dating of picked, monospecific samples of the planktonic foraminifer *Globigerinoides bulloides* over 18 levels spanning the last 23 cal. ka BP. Analyses were conducted at the Center for Accelerator Mass Spectrometry (CAMS) facility at Lawrence Livermore National Laboratory. Between 1000 and 1500 *G. bulloides* individuals were picked from the $> 150 \mu\text{m}$ fraction of each sample and individual samples were sonicated in dionized water several times and leached in dilute HCl prior to AMS radiocarbon analysis. The precise reservoir correction to be applied for this region is uncertain but should be larger than the surface ocean average of 400 yr due to the upwelling of older subsurface waters, so we used a conservative reservoir correction of 500 yr which was subtracted from the raw radiocarbon ages. Additional ^{14}C ages measured on *G. inflata* were consistently younger than ages obtained for *G. bulloides* in the same sample (by 400–600 yr, (Knaack, 1997; Papenfuss, 1999)), so the *G. bulloides* ages listed in Table 1 must be considered maximum age estimates. Corrected radiocarbon ages were calibrated to calendar ages using the Calib 3.03 program (Stuiver and Reimer, 1993); the radiocarbon dates and calibrated ages (with ± 2 sigma ranges) are listed in Table 1. Dates and ages referred to in this paper are calibrated calendar ages (rounded to the nearest decade) unless otherwise specified.

658C - West Africa

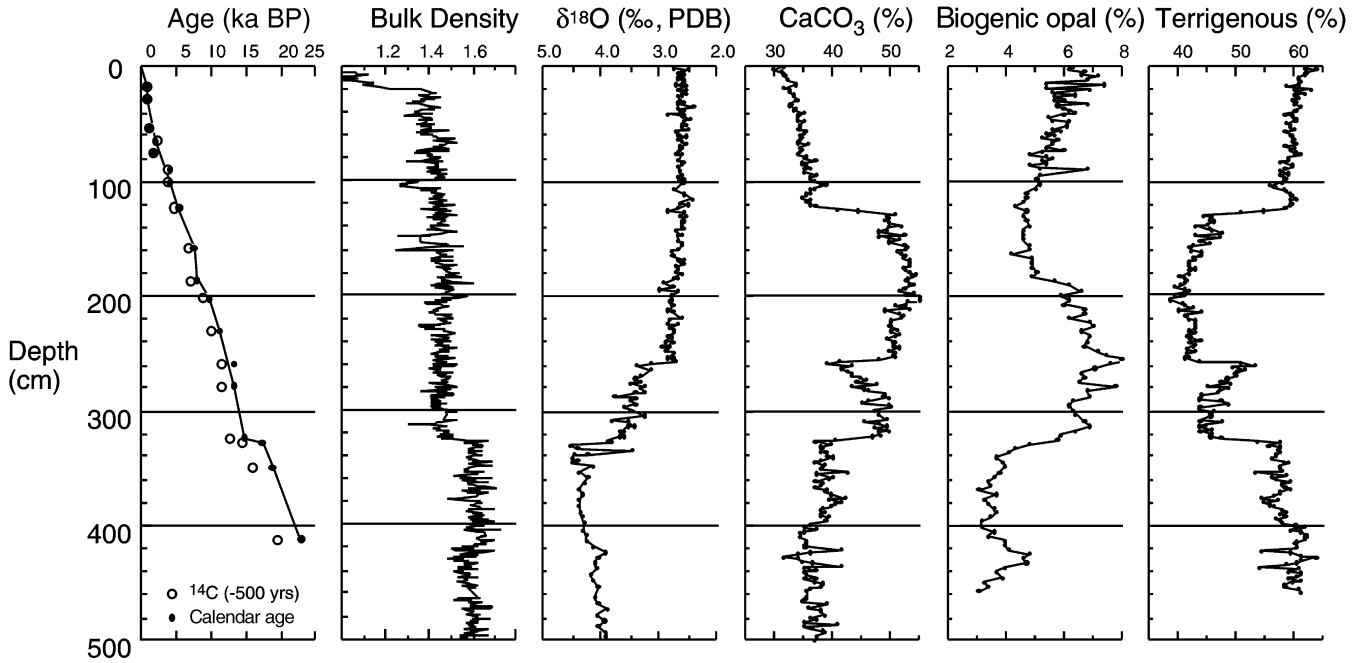


Fig. 2. Sediment composition data and AMS radiocarbon age control from Site 658C. Samples were taken continuously at 2 cm intervals, which is roughly equivalent to 50–150 yr based on the 18 cm/ka average sedimentation rates at Site 658C. A brief hiatus between 14.8 and 17.2 cal. ka BP is indicated by two closely spaced AMS radiocarbon dates at 324 and 328 cm (Table 1). Note the very abrupt changes in sediment composition which occur at 326 cm (ca. 14.8 cal. ka BP), 260 cm (12.3 cal. ka BP), and 125 cm (ca. 5.5 cal. ka BP).

Table 1

AMS radiocarbon dating of Site 658C planktonic foraminifera. All values were measured at the Center for Accelerator Mass Spectrometry (CAMS) at the Lawrence Livermore National Laboratory. Samples of between 1000 and 1500 picked, monospecific planktonic foraminifera (*G. bulloides*) were sonicated in deionized water prior to analysis. Calibrated ages were rounded to the nearest decade (Stuiver and Reimer, 1993)

Site/core/type/sect./depth1 & 2	Depth (cm)	Species	14 C age (yr BP)	± error	14 C age (yr, corr. ^b)	Calib. Age (yr BP)	2-sigma calib. age range
658C ^a 1 H 1 16 18 17		<i>G. bulloides</i>	1130	50	630	600	549–653
658C 1 H 1 28 30 29		<i>G. bulloides</i>	1390	40	890	780	732–899
658C 1 H 1 52 54 53		<i>G. bulloides</i>	1600	40	1100	980	952–1057
658C 1 H 1 64 66 65		<i>G. bulloides</i>	2550	40	2050	1990	1944–2040
658C 1 H 1 74 76 75		<i>G. bulloides</i>	2100	40	1600	(1510)	1393–1555
658C 1 H 1 88 90 89		<i>G. bulloides</i>	4290	40	3790	4150	4088–4230
658C 1 H 1 100 102 101		<i>G. bulloides</i>	4220	40	3720	4030	3983–4092
658C ^a 1 H 1 122 124 123		<i>G. bulloides</i>	5080	40	4580	5300	5098–5313
658C 1 H 2 4 6 158		<i>G. bulloides</i>	7100	40	6600	7470	7393–7518
658C 1 H 2 32 34 186		<i>G. bulloides</i>	7590	40	7090	7850	7826–7918
658C 1 H 2 48 50 202		<i>G. bulloides</i>	9280	60	8780	9710	9650–9885
658C 1 H 2 76 78 230		<i>G. bulloides</i>	10 520	40	10 020	11 210	11 047–11 646
658C 1 H 2 105 107 259		<i>G. bulloides</i>	11 780	40	11 280	13 190	13 122–13 260
658C 1 H 2 124 126 278		<i>G. bulloides</i>	11 780	40	11 280	13 190	13 122–13 260
658C ^a 1 H 3 16 18 324		<i>G. bulloides</i>	13 030	40	12 530	14 690	14 518–14 873
658C ^a 1 H 3 20 22 328		<i>G. bulloides</i>	14 860	60	14 360	17 210	17 103–17 320
658C 1 H 3 42 44 350		<i>G. bulloides</i>	16 490	80	15 990	18 870	18 749–18 992
658C ^a 1 H 3 104 106 412		<i>G. bulloides</i>	19 960	80	19 460	22 910	

^aDates used to constrain the “nominal” age model (see text).

^bRadiocarbon ages after 500 year reserver corection.

4. Results

The radiocarbon age model shown in Fig. 2 indicates a very high average sedimentation rate at Site 658C of approximately 18 cm/ka. The AMS ^{14}C dates increase monotonically with depth with the exception of one age reversal at 89 cm (Fig. 2). The age control data do indicate that sedimentation was continuous spanning the last ca. 15 ka. However, a nondepositional or erosional hiatus is indicated for the interval from 17.20 to 14.80 cal. ka BP by two closely dated samples at 328 cm (17.21 cal. ka BP) and 324 cm (14.69 cal. ka BP). A hiatus at this level was also suggested by early radiocarbon results by Knaack (1997) and Papenfuss (1999). That this hiatus is stratigraphically abrupt is supported by the step-like increase bulk density and the sharp 0.7‰ increase in $\delta^{18}\text{O}$ which occurs across this 328–324 cm interval (Fig. 2). The hiatus appears to be bounded by these dates and thus spans the first phase of the last deglaciation between 14.80 and 17.20 cal. ka BP. The hiatus may have been attributable to a coring artifact resulting from post-

recovery gas expansion (Ruddiman et al., 1988). There are no other similarly sharp inflections in the radiocarbon age model to suggest other hiatuses in the 658C record.

The Site 658C composition data document rapid and large-amplitude changes in sediment composition which occurred during the latest Pleistocene and Holocene (Figs. 2 and 3). Three major compositional shifts occurred over the last ca. 20 cal. ka BP which are centered at depths of 324 cm (14.65 cal. ka BP), 260 cm (12.32 cal. ka BP), and 125 cm (5.49 cal. ka BP) (Figs. 2 and 3). Working from the base of the Site 658C section upwards, there is a dramatic increase in biogenic carbonate and opal (and decrease in terrigenous (eolian) sediment) which occurs between 324 cm and 126 cm (14.65–5.49 cal. ka BP). This 14.65–5.49 cal. ka BP interval of lower terrigenous percentages was punctuated by a brief but sharp increase (decrease) in terrigenous (carbonate) sediment concentrations between 284 and 257 cm (ca. 13.38–12.32 cal. ka BP) which is roughly contemporaneous with the Younger Dryas period). The sediment compositional

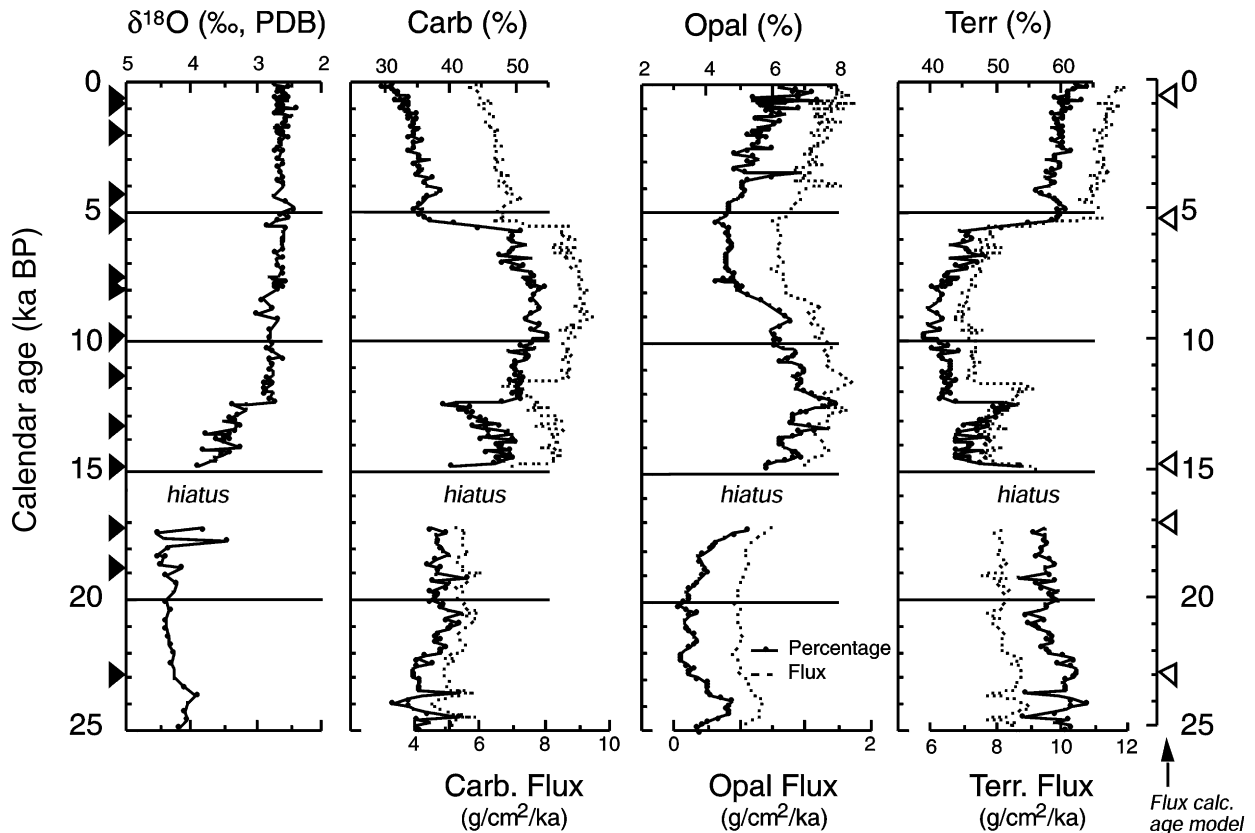


Fig. 3. Biogenic carbonate, opal and terrigenous sediment percentage and flux records (dashed lines, in $\text{g}/\text{cm}^2/\text{ka}$) from Site 658C. Eighteen AMS radiocarbon dates were used to constrain the carbonate, opal, and terrigenous percentage time series; age control points are indicated by filled triangle symbols to the left of the figure. Radiocarbon ages were converted to calibrated calendar ages using the Calib 3.03 program (Stuiver and Reimer, 1993) after applying a 500 yr reservoir correction to the raw ^{14}C ages. Flux data were calculated using the “nominal” age model derived from a subset of ^{14}C age control levels. Flux data are shown by dashed lines and the nominal age control points are shown by open triangles to the right of the figure. Note the abruptness of the 14.8, 12.3, and 5.5 cal. ka BP sediment composition transitions, each of which were completed within several centuries.

Table 2
Mean sediment component accumulation rates at Site 658C

Age interval	Carbonate (g/cm ² /ka)	Opal (g/cm ² /ka)	Terrigenous (g/cm ² /ka)	Total (g/cm ² /ka)
0–5.2 ka	6.46 (34%)	1.06 (6%)	11.22 (60%)	18.75
5.3–14.8 ka	8.45 (49%)	1.04 (6%)	7.64 (45%)	17.12
17.2–26.0 ka	5.3 (37%)	0.54 (4%)	8.30 (59%)	14.15

timeseries shown in Fig. 3 were constrained using the calibrated radiocarbon dates listed in Table 1.

4.1. Sediment flux variations at Site 658C

Were these abrupt compositional shifts attributed to changes in terrigenous or carbonate sediment supply? Using the calibrated radiocarbon age model listed in Table 1 we computed the mass flux (in g/cm²/ka) for each constituent by computing the vector product of interval sedimentation rates, fractional abundance of each constituent, and dry bulk density (Fig. 3). The actual sedimentation rate profile at Site 658 is most likely much more complex than can be captured by the 18 AMS dates, so we computed the average component accumulation rates for the three main intervals which show large compositional differences: 26.0–17.2, 14.8–5.5, and 5.5–0 cal. ka BP (Table 2). This “nominal” age model is only used to estimate large-scale changes in sediment influxes of biogenic and terrigenous components summarized in Table 2. It is immediately apparent that the Site 658C sediment fluxes are much larger than typical pelagic ocean sediments due to highly productive surface waters and high supply of terrigenous eolian sediment. Average terrigenous sediment fluxes at Site 658C are roughly 10 times larger than the more distal ODP Site 659 off West Africa (Tiedemann et al., 1994), which is consistent with the log-normal mass-distance particle fallout relationship for atmospheric aerosols (Pye, 1987; Schütz et al., 1981).

The abrupt increase in terrigenous percent which occurred at ca. 5.5 cal. ka BP can be attributed to the nearly 50% increase in terrigenous sediment flux across this transition (Fig. 3). The influx of detrital, predominantly African eolian sediment increased 47% from 7.6 to 11.2 g/cm²/ka, whereas the biogenic carbonate flux decreased 24% across the 5.5 cal. ka BP transition. The abrupt decrease in terrigenous percent which occurred near 14.8 cal. ka BP can mainly be attributed to an increase in the supply of biogenic carbonate sediments which increase 59% from 5.31 to 8.5 g/cm²/ka; terrigenous flux decreased 8% from 8.3 to 7.6 g/cm²/ka (Table 2). The component flux changes which we have calculated across the 14.8 cal. ka BP transition must be considered preliminary and subject to modification since the hiatus needs to be more firmly bounded by additional AMS dates. Although the terrigenous flux variations broadly mirror the

terrigenous percentage data (Fig. 3), changes in carbonate flux due to changes in productivity or preservation are also important at Site 658C.

4.2. Abruptness of the sediment composition changes

These climatic transitions were very abrupt and were evidently completed within a few centuries. These transition times must be considered maximum estimates as they were derived from radiocarbon dates of a non-laminated marine sediment sequence, neither of which have the temporal resolution to absolutely date precisely decadal-century scale transitions. However, the high sedimentation rates provide the necessary relative time resolution for constraining century-scale climatic jumps at Site 658C. Using all radiocarbon age control data, we estimate that the ca. 5.5 cal. ka BP increase in terrigenous (eolian) sediment supply occurred in less than four centuries centered at 5490 ± 190 yr BP (4780 ¹⁴C yr BP). The termination of the Younger Dryas arid period is dated in this core at 12.3 cal. ka BP and evidently occurred in less than two centuries (Fig. 3). The abrupt decrease in terrigenous percent at ca. 14.8 cal. ka BP evidently occurred rapidly as well and is centered at $14,785 \pm 90$ yr BP (12,630 ¹⁴C yr BP). We cannot be certain at this point that this 14.8 cal. ka BP transition is stratigraphically distinct from the hiatus, but several lines of evidence suggest that the hiatus occurs just below the transition. A calibrated AMS radiocarbon date of 14,692 yr BP was obtained for the 324 cm sample, which occurred stratigraphically within the transition (Figs. 2–4, Table 1), suggesting that the transition itself is intact and distinct from the hiatus. Furthermore, the 14.8 cal. ka BP date agrees extremely well with the onset of humid conditions in Africa derived from a variety of independent paleoclimatic data sources (see below) (Sarnthein et al., 1994; Johnson et al., 1996; Sowers and Bender, 1995; Street and Grove, 1979).

4.3. The Site 658C record of eolian deposition and comparison with African terrestrial paleoclimate records

The calibrated dates for the subtropical African climate shifts recorded at Site 658C agree with terrestrial and marine paleoclimate records of the onset and termination of the African Humid Period and the Younger

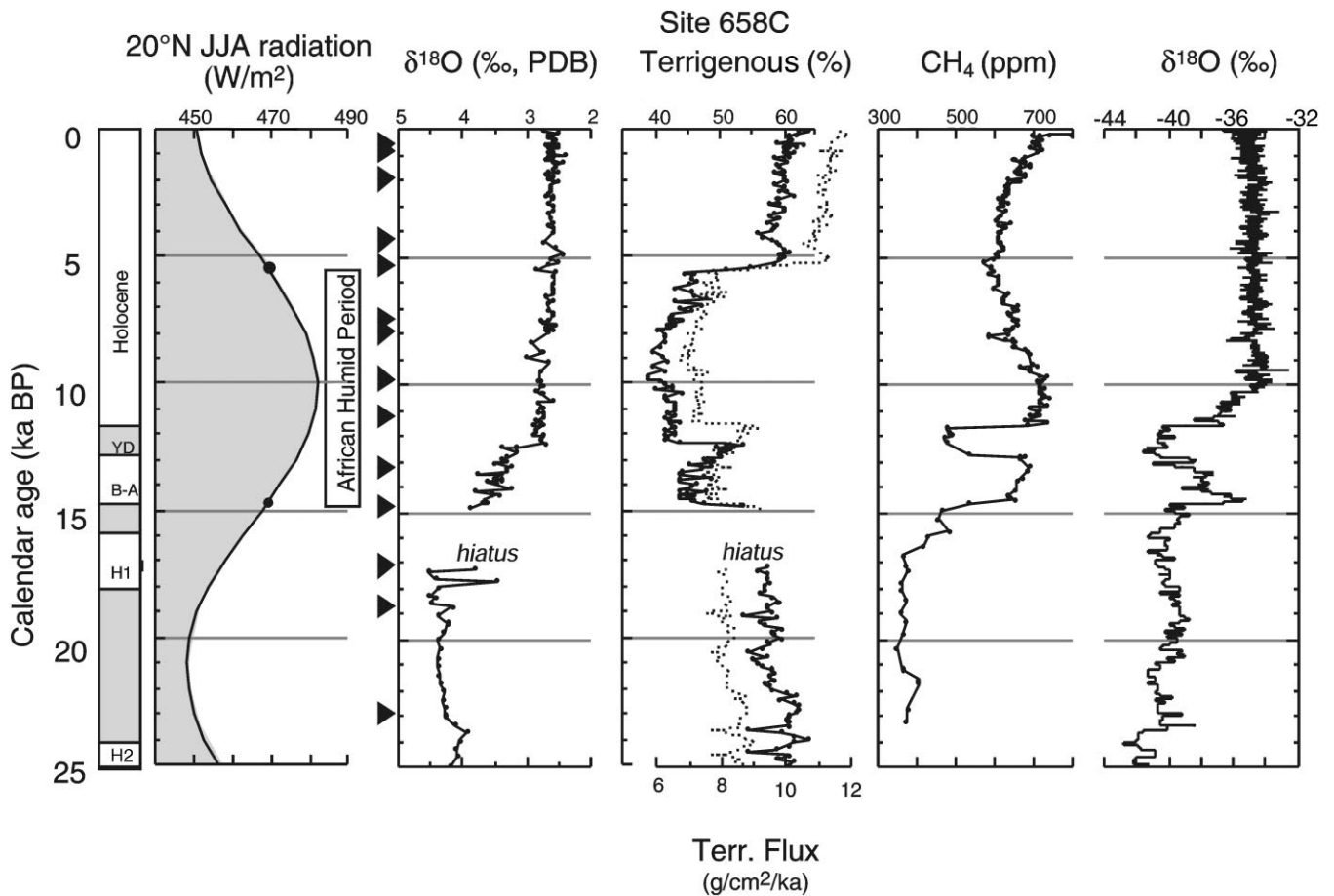


Fig. 4. Comparison of the boreal summer (JJA) average insolation computed for 20°N (Berger and Loutre, 1991) with the Site 658C benthic oxygen isotope record (from analyses of *C. wuellerstorfi*), and terrigenous (eolian) percentage and flux records spanning the last 25 cal. ka BP. Note the onset and termination of the African Humid Period in terms of the low eolian dust flux at Site 658C between ca. 14.8 ka and 5.5 cal. ka BP associated with the early Holocene rise in summer insolation forcing of the African monsoon. Atmospheric methane concentrations preserved in occluded ice bubbles and the oxygen isotopic composition of glacial ice in the GISP2 Greenland ice core are also shown (Blunier et al., 1995; Dansgaard, 1993). The onset of the African Humid Period was synchronous with the end of cold, glacial conditions in Europe, which occurred by ca. 14.5 cal. ka BP, corresponding to the end of Heinrich event 1 in the North Atlantic (Blunier et al., 1995; Bond et al., 1993; Broecker et al., 1993; Dansgaard, 1993). The rapid onset of humid conditions in the tropics is also recorded by the abrupt increase in atmospheric methane at ca. 14.7 cal. ka BP, which documents the rapid expansion of tropical wetland methane sources (Blunier et al., 1995). The Site 658C data confirm terrestrial African paleoclimate records which document a brief (ca. 1 ka) interval of more arid conditions associated with the cool Younger Dryas Chronozone (Gasse et al., 1989; Gasse et al., 1990; Roberts et al., 1993; Street-Perrott and Perrott, 1990; Williamson et al., 1993). The termination of the African Humid Period at 5.5 cal. ka BP coincides with the mid-Holocene minimum in atmospheric methane concentration. The subsequent late Holocene methane rise has been attributed to the expansion of boreal wetlands which were absent during the first stages of the deglaciation (Blunier et al., 1995). The timing of the terrigenous transitions at ca. 5.5 and 14.8 cal. ka BP are indicated on the JJA insolation curve (filled symbols).

Dryas cool period. A survey of subtropical African paleolakes documents that lake basins in the hyperarid to arid regions began to fill and expand near 14.5 cal. ka BP (Street and Grove, 1979; Street-Perrott and Harrison, 1984; Gasse, 1999). Radiocarbon dates on piston cores recovered from Lake Victoria firmly place the onset of lacustrine deposition there at 14,500 yr BP ($12,400 \pm 70$ ¹⁴C yr BP) following late Pleistocene aridity and complete desiccation (Johnson et al., 1996). Additionally, the record of atmospheric methane variability recorded in ice bubbles trapped in the Greenland ice cores documents a very abrupt increase in global atmospheric methane

concentrations, probably reflecting a dramatic increase tropical wetland CH₄ production which commenced at 14.7 cal. ka BP (Fig. 4) (Blunier et al., 1995; Sowers and Bender, 1995). The onset of the African Humid Period was synchronous with the end of cold, glacial conditions in Europe and the North Atlantic – Heinrich event 1 — which occurred by ca. 14.5 cal. ka BP (Blunier et al., 1995; Bond et al., 1993; Broecker et al., 1993; Dansgaard, 1993).

The Younger Dryas period is formally known in Europe and the North Atlantic as a return to cold, near-glacial conditions between ca. 12.5 and 11.5 cal. ka BP (Broecker

et al., 1988; Mangerud, 1987; Roberts, 1998; Alley et al., 1999 this issue). In subtropical Africa, the Younger Dryas period has been associated with a sharp increase in regional aridity which interrupted the African Humid Period (Gasse et al., 1989; Gasse et al., 1990; Roberts et al., 1993; Street-Perrott and Perrott, 1990; Williamson et al., 1993; Gasse, 1999 this issue). The record of terrigenous (eolian) sedimentation at Site 658C documents a brief (1 ka) interval of enhanced aridity (increased eolian transport) which is dated between 13.4–12.3 cal. ka BP (Figs. 3, 4). This event in Site 658C would appear to slightly precede (by 800 yr) the well-constrained range of the Younger Dryas event. As mentioned in the methods section, our *G. bulloides* radiocarbon ages were consistently older than ages determined for *G. inflata* within the same samples (Knaack, 1997; Papenfuss, 1999), so the *G. bulloides* ages must be considered as maximum age estimates. Additionally, the marine ^{14}C reservoir correction was nearly twice as large as the modern value during the Younger Dryas (700 yr vs. 400 yr) due to changes in deep ocean circulation and related changes in ocean-atmosphere radiocarbon partitioning (Austin et al., 1995; Bard et al., 1994; Oeschger et al., 1980). Furthermore, foraminiferal assemblage changes at Site 658C document large increases in *G. bulloides* abundances over the 14.8–5.5 cal. ka BP interval (including the Younger Dryas interval; P. deMenocal, unpub. data), which would be consistent with increased regional upwelling and older apparent ^{14}C ages at this time. Together, these factors would have been sufficient to increase the local apparent reservoir age correction of the Younger Dryas event to ~800–900 yr at Site 658C.

Terrestrial paleoclimate records indicate that there was an abrupt onset of more arid conditions in subtropical North Africa near 8.2 cal. ka BP (Alley et al., 1997; Gasse and Van Campo, 1994). The development of more arid conditions at this time spanned from subtropical Africa to southeast Asia, and is contemporaneous with a sharp, short-lived cooling event in the North Atlantic and Greenland Alley et al., 1997; Gasse and Van Campo, 1994). At Site 658C, terrigenous sediment accumulation increased sharply after ca. 8 cal. ka BP (Figs. 3, 4), marking a transition toward more arid conditions. However, in contrast to the African and high-latitude paleoclimate records, the sediment transition at Site 658C was not particularly abrupt nor short-lived. The Site 658C record suggests that the 8.2 cal. ka BP event marked the end of the most humid conditions in subtropical Africa, with a gradual decline in the precipitation-evaporation balance which culminated in the very abrupt onset of much more arid conditions at 5.5 cal. ka BP. Planktonic foraminiferal assemblage variations at the ca. 8 cal. ka BP level at Site 658C indicate an abrupt and short-lived cooling event which was the coolest period of the entire Holocene, being nearly 6–8°C cooler than modern values (deMenocal, unpub. data).

The end of the African Humid Period was very abrupt, having been completed within several centuries. The onset of more arid conditions and the contraction of lake basins evidently occurred across subtropical Africa between 6 and 5 cal. ka BP (Gasse and Van Campo, 1994; Jäkel, 1979; Munson, 1981; Pachur and Altman, 1997; Petit-Maire and Guo, 1996; Roberts, et al., 1994; Sarnthein, 1978; Talbot and Delbrias, 1980; Talbot, 1980; Gasse, 1999). The timing of the lake level lowerings associated with this event are broadly clustered between 6–5 cal. ka BP, but evidently show some basin-to-basin variability in the timing of this shift to more arid conditions (Street-Perrott and Harrison, 1984). The absence of a similarly abrupt decrease in atmospheric CH_4 at this time has been interpreted to reflect the gradual Holocene emergence and expansion of boreal wetlands which were absent during the first stages of the deglaciation (Blunier et al., 1995). The mid-Holocene minimum in atmospheric CH_4 concentrations near 5.5–5.0 cal. ka BP (Fig. 4) has been interpreted to reflect the loss of this subtropical methane source (Blunier et al., 1995). The subsequent late Holocene methane rise has been attributed to the expansion of boreal wetlands which were absent during the first stages of the deglaciation (Blunier et al., 1995). Many studies have shown that the primary aridification event began between 6–5 cal. ka BP, followed by a brief return to humid conditions near 4 cal. ka BP (see McIntosh and McIntosh, 1983; Petit-Maire et al., 1987). The Site 658C terrigenous record exhibits a subsequent, but short-lived reduction in terrigenous sedimentation centered at 4.3–4.1 cal. ka BP which may be synchronous with this humid period (Fig. 4).

5. Discussion

Early investigations into the late Pleistocene–Holocene evolution of African climate recognized the paleoclimatic significance of these abrupt arid-humid transitions (Faure et al., 1963). The geologic evidence for the onset and collapse of the African Humid Period is so striking that these events have been termed “climatic crises”, acknowledging the sheer magnitude and spatial scale of these climatic events (Rognon, 1983). The collective contribution of decades of African paleoclimatic data now bears witness to a century-scale replacement of a once verdant, lake-dotted, and populated landscape by the now-hyperarid desert largely devoid of vegetation and life. Our results from Site 658C suggest that this and other transitions occurred extremely abruptly, within a few decades to centuries.

5.1. Timing of the African Humid Period relative to orbital insolation forcing

One of the most striking features of the Site 658C terrigenous record beyond the abruptness of the climate

transitions is the timing of the transitions themselves relative to the orbital insolation forcing. Boreal summer insolation was calculated for the boreal summer season (JJA) at 20°N, the latitude of maximum sensible heating over subtropical West Africa (Webster, 1987; Berger and Loutre, 1991). As shown in Fig. 4, the onset and termination of the African Humid Period near 14.8 and 5.5 cal. ka BP occurred at nearly identical summer insolation values of 470 W/m², which is roughly 4.2% above the modern value of 451 W/m². This observation may indicate a climate threshold response, whereby subtropical African climate flips abruptly between humid and arid modes as summer radiation, the primary forcing of the summer monsoon, passes a critical value. As described below, fully coupled (ocean–atmosphere–vegetation) climate model simulations of the African monsoon suggest that there are two stable solutions of the Saharan region (vegetated vs. non-vegetated) to prescribed orbital insolation boundary condition changes (see Claussen et al., 1999; Brovkin et al., 1998). Furthermore, these climate models also indicate that the arid-humid transition occurs at the same orbital insolation threshold.

What changes in subtropical ocean–atmosphere climate dynamics led to such an abrupt climate response to the gradual, periodic insolation forcing of the African monsoon? Are these transitions reflective of a threshold response and, if so, what are the attractors? Climate model simulations provide a useful context for studying the dynamical processes that affect the seasonal timing and amplitude of the monsoon, as well as its coupled sensitivity to associated changes in regional vegetation and surface ocean responses. Here, we consider climate model investigations into the sensitivity of monsoonal climate to prescribed changes in insolation forcing alone, and then we assess the additional responses resulting from associated (coupled) changes in surface ocean temperatures, African vegetation and surface hydrologic budgets, and, finally, we discuss the response of fully coupled ocean–atmosphere–vegetation models to the initial orbital radiation forcing.

5.2. Atmosphere-only and coupled climate model simulations of the mid-Holocene African monsoon

Early climate modeling efforts using uncoupled, atmosphere-only general circulation models (GCMs) indicate that while the African monsoon system is very responsive to insolation forcing, the response is strongly linear. Using the NCAR-CCM1 climate model, Prell and Kutzbach (1987) found that the 8% relative increase in summer insolation due to earth orbital geometries at ca. 10 cal. ka BP produced a roughly 40% increase in subtropical African monsoonal precipitation (Fig. 5). This five-fold gain between insolation forcing and monsoonal precipitation was found to be highly linear for the full late Pleistocene range of orbital configurations (e.g. between

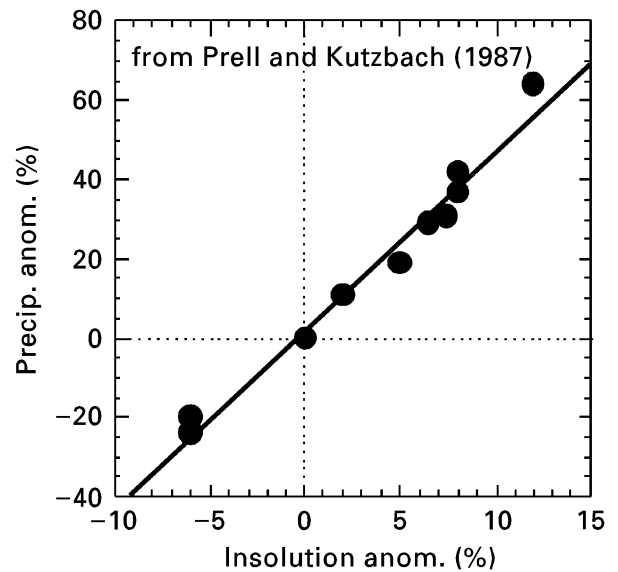


Fig. 5. The linear relationship between orbital insolation forcing and simulated changes in African monsoonal precipitation using an atmosphere-only climate model which does not employ coupled ocean and/or vegetation feedbacks (from Prell and Kutzbach, 1987). The monsoon is strongly linked to orbital changes in seasonal radiation forcing, but there is no indication of non-linear or threshold responses from these early atmosphere-only experiments. Strongly positive, non-linear amplifications of the primary insolation forcing of monsoonal climate are achieved in climate model simulations which explicitly include coupled vegetation, land surface processes, and surface ocean responses (see text).

– 5 to + 15% of modern summer radiation). These results are generally consistent with the paleoclimate data, although the simulated P-E budget would not have been sufficient to form and sustain the large, perennial lakes which are known to have existed across the Sahara and Sahel regions during the early to mid-Holocene (Broström et al., 1998; Coe and Bonan, 1997; Kutzbach, 1996). A paradigm which arose from these early simulations is that monsoonal circulation is essentially a heat engine which responds *linearly* to prescribed radiation changes.

5.3. Effects of vegetation and land-surface feedbacks on African monsoonal climate

Subsequent climate modeling studies have explicitly examined how monsoonal climate sensitivity is affected by formally incorporating coupled vegetation and/or coupled ocean model elements. Using an asynchronously coupled ocean–atmosphere GCM, Kutzbach and Liu (1997) found that the increased mid-Holocene summer radiation also increased surface ocean temperatures (by 0.4°C) which further increased summer African monsoonal precipitation by 25% over uncoupled, atmosphere-only simulations. Similar conclusions have been described by Hewitt and Mitchell (1998) using the

Hadley Centre synchronously coupled ocean-atmosphere GCM (HADCM2). In these experiments, the monsoon was both greatly intensified due to increased moisture advection from the warmer surface ocean, and rains penetrated much deeper into the North African interior (and later into the year) relative to the uncoupled simulations (Hewitt and Mitchell, 1998; Kutzbach and Liu, 1997). Although these experiments were not able to produce the monsoon intensification required to match mid-Holocene paleoclimate data (e.g. abundant perennial lakes throughout the present-day expanse of the Sahara Desert), the surface ocean feedbacks were positive and large.

A separate set of climate model studies have explicitly considered the effects of prescribed and coupled changes in African vegetation and surface water on the strength of the African monsoon; these feedbacks were also positive and large (Brovkin et al., 1998; Coe and Bonan, 1997; Foley, 1994; Hoelzmann et al., 1998; Kutzbach, 1996). Idealized studies have shown that prescribed changes in African vegetation can increase monsoonal precipitation to levels which are roughly equal to the increases due to orbital radiation forcing alone. Kutzbach (1996) employed a coupled atmosphere-vegetation GCM in series of experiments to explore how changes in vegetation and soil type affected the response of the African monsoon to insolation forcing. He found that the prescribed replacement of desert with grassland vegetation, and of desert soils with loamy soils resulted in separate precipitation increases of 6 and 10%, respectively, as compared to the radiation-only precipitation increase of 12%. Coe and Bonan (1997) investigated the effect of prescribed mid-Holocene increases in surface water coverage (lakes and wetlands) over northern Africa and found, too, that the monsoonal circulation was enhanced due to associated changes in the surface albedo and latent heat budgets. Broström et al. (1998) found that prescribing mid-Holocene land-surface conditions in their coupled atmosphere-land surface climate model prolonged the monsoon season by two months and caused it to penetrate nearly 300 km further into north Africa.

5.4. Abrupt mid-Holocene shift in subtropical African climate simulated by a fully coupled atmosphere-ocean-vegetation climate model

All of the climate models described thus far are too complex to be run as transient experiments for many thousands of model years to quantify time-dependent changes in the coupled ocean-atmosphere-vegetation responses to the initial insolation forcing. Ganopolski et al. (1998) report the application of the Climate and Biosphere (CLIMBER) model, a zonally averaged, coupled ocean-atmosphere model with an equilibrium vegetative subsystem. The model is computationally efficient and it

can be used to explore transient changes in ocean-atmosphere-vegetation feedbacks over many millennia. The model has very coarse ($10^\circ \times 51^\circ$) spatial resolution and consists of a 2.5-dimensional dynamical-statistical atmospheric model coupled to a multibasin, zonally averaged ocean model with responsive sea-ice, and a terrestrial vegetation parameterization that responds to growing degree days and precipitation. Fractional vegetation types are permitted within gridboxes so that the effective resolution of the vegetative model is greater than the model resolution (Ganopolski et al., 1998). The model was later modified (CLIMBER2) to include dynamic (diagnostic) vegetation responses to surface climate changes (Brovkin et al., 1998; Claussen et al., 1999).

The CLIMBER2 model was configured for a transient simulation of the last 9000 yr of the Holocene, being forced only by the gradual changes in incident summer season radiation due earth orbital variations (Claussen et al., 1999). CLIMBER2 simulates an abrupt termination of the African Humid Period centered at 5450 yr BP in response to the gradual drop in insolation from 9000 yr. BP to the present (Fig. 6a–c). The humid-arid transition occurs abruptly, within several centuries (Fig. 6b,c). The timing of the climate model transition was stable, occurring at 5440 ± 30 yr, based on an average of 10 separate simulations that differed only in the initial conditions but were otherwise forced by the same insolation series (Claussen et al., 1999). The timing and shape of this modeled transition compare favorably with the abrupt mid-Holocene increase in eolian dust supply at Site 658C centered at 5490 ± 190 yr BP (4780 ^{14}C yr BP) (Fig. 6d).

The abruptness of the Claussen et al. (1999) modeled climate transition was attributed to the vegetation sensitivity to changing precipitation fields associated with the gradually decreasing insolation forcing of the monsoon (Claussen et al., 1999). Atmosphere-only, and coupled ocean-atmosphere simulations that lack responsive vegetation exhibited smooth climatic responses to the gradual orbital forcing (Claussen et al., 1999). The abrupt climate response to gradual insolation forcing in this model can be attributed to the positive feedbacks which link changes subtropical vegetation, albedo, and precipitation. The gradually decreasing monsoonal precipitation leads to decreases in vegetation cover which raise the surface albedo as desert sands become increasingly prevalent, thereby reducing the efficiency of the initial radiation forcing of the monsoon. As demonstrated with fully coupled model experiments, the individual effects of vegetation and land-surface feedbacks can far exceed the fundamental radiation sensitivity of monsoonal climate (Broström et al., 1998; Brovkin et al., 1998; Coe and Bonan, 1997; Foley, 1994; Hewitt and Mitchell, 1998; Hoelzmann et al., 1998; Kutzbach, 1996; Kutzbach and Liu, 1997).

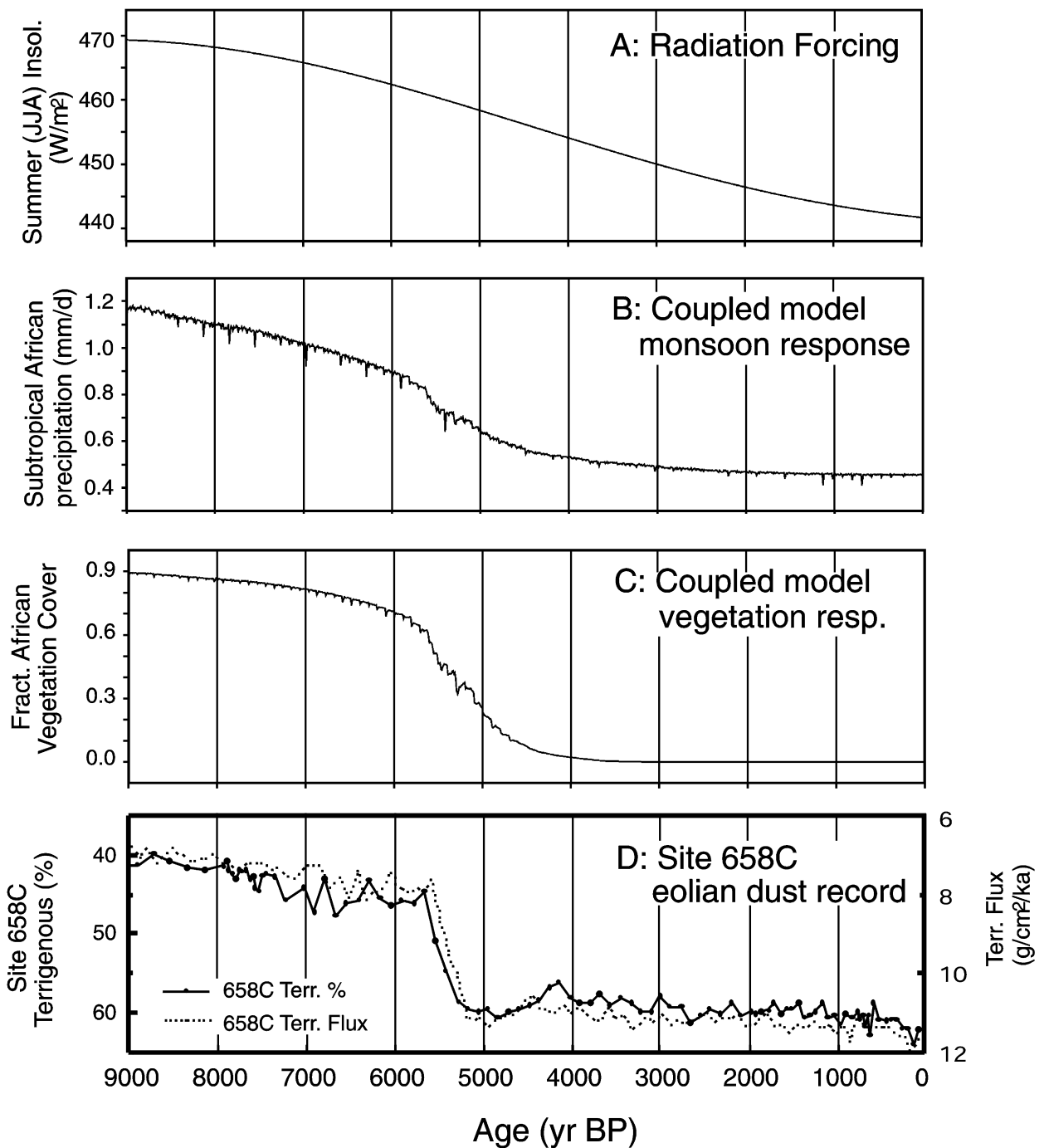


Fig. 6. Average Northern Hemisphere summer insolation (JJA, in W/m^2) used to force the coupled ocean–atmosphere–vegetation CLIMBER2 model for the 9 000 yr BP to present transient simulation of Holocene changes in subtropical African climate (Claussen et al., 1999) (a). In the fully coupled model, annual Saharan precipitation (b) and fractional Saharan vegetation cover (c) decreases very abruptly at 5440 ± 30 yr BP (based on an ensemble average of 10 separate transient simulations; (Claussen et al., 1999)). The abrupt African climate responses were attributed to the highly non-linear (positive) feedbacks linking progressive decreases in regional precipitation, vegetation cover loss, and increasing albedo (Claussen et al., 1999). Note the remarkable similarity between the shape and timing of the abrupt mid-Holocene termination of the African Humid Period at 5.5 cal. ka BP for the climate model simulation (b), (c) and the Site 658C record of West African eolian dust supply variations (d).

6. Conclusions

The record of terrigenous (eolian) sedimentation at West African Site 658C documents the very abrupt onset

and termination of the African Humid period near 14.8 and 5.5 cal. ka BP, respectively. These transitions apparently occurred within several decades to centuries, and were much too rapid to be driven by a simple linear

responses to gradual insolation forcing. Current climate modeling results suggest two (positive) feedback processes that may have been important factors contributing to the abruptness of these transitions: Coupled vegetation-albedo feedback and surface ocean temperature-moisture transport feedback. These processes can “rectify” the sinusoidal orbital forcing signal to produce the square-wave climate response signal we see at Site 658C and in terrestrial African paleoclimate records of abrupt climatic change (Figs. 4 and 6). The timing of the transitions themselves relative to insolation forcing indicates that they occurred when summer insolation crossed a threshold value of 470 W/m^2 , which is roughly 4.2% above modern values. The abruptness of these climate transitions at Site 658C suggest that this rectification process is both very effective and very stable. These feedback processes interact with primary (e.g. radiation) forcing to lock subtropical African climate into one of two (vegetated vs. non-vegetated) stable equilibrium climatic solutions (Claussen et al., 1998). As such, the subtropical monsoon climate system may be viewed as a low-latitude corollary to the well-documented, bi-stable behavior of high-latitude deep ocean thermohaline circulation (Broecker, 1994; Broecker, et al., 1985; Manabe and Stouffer, 1988; Rahmstorf, 1995; Stocker et al., 1992).

Acknowledgements

The authors would like to thank John Miller and Paula Weiss from the Ocean Drilling Program for their help in the detailed sampling Site 658C. Helpful comments and significant input to this paper were contributed by Bob Anderson, Andre Berger, Martin Claussen, Claude Hillaire-Marcel, George Kukla, and David Rind. Comments by two anonymous reviewers greatly improved the final manuscript. This project was supported by the Marine Geology and Geophysics division of the National Science Foundation. This is LDEO contribution number 5961.

References

- Alley, R.B., Mayewski, P.A., Sowers, T., Stuiver, M., Taylor, K.C., Clark, P.U., 1997. Holocene climatic instability: a prominent, widespread event 8200 yr ago. *Geology* 25 (6), 483–486.
- Alley et al. 1999. The Younger Dryas cold interval as viewed from central Greenland *Quaternary Science Reviews*, 19, this issue.
- Anderson, D.M., Prell, W.L., 1992. The structure of the southwest monsoon winds over the Arabian Sea: observations, simulations, and marine geological evidence. *Journal of Geophysical Research* 97 (C10), 15481–15487.
- Austin, W.E., Bard, E., Hunt, J.B., Kroon, D., Peacock, J.D., 1995. The ^{14}C age of the Icelandic Vedde Ash: Implications for Younger Dryas marine reservoir corrections. *Radiocarbon* 37 (1), 53–62.
- Bard, E., Arnad, M., Mangerud, J., Pateine, M., Labeyrie, L., Duprat, J., Melieres, M.A., Sonstegaard, E., Duplessy, J.-C., 1994. The North Atlantic atmosphere-sea surface ^{14}C gradient during the Younger Dryas climatic event. *Earth and Planetary Science Letters* 126, 275–287.
- Berger, A., Loutre, M.F., 1991. Insolation values for the climate of the last 10 million years. *Quaternary Science Reviews* 10, 297–317.
- Blunier, T., Chappellaz, J., Schwander, J., Stauffer, B., Raynaud, D., 1995. Variations in atmospheric methane concentration during the Holocene epoch. *Nature* 374, 46–49.
- Bond, G., Broecker, W.S., Johnsen, S., McManus, J., Labeyrie, L., Jouzel, J., Bonani, G., 1993. Correlations between climate records from North Atlantic sediments and Greenland ice. *Nature* 365, 143–147.
- Broecker, W., Bond, G., McManus, J., 1993. Heinrich event triggers of ocean circulation change? In: Peltier, W.R. (Ed.), *Ice in the Climate System*. Springer-Verlag, Berlin, pp. 161–166.
- Broecker, W.S., 1994. An unstable superconveyor. *Nature* 367, 414–415.
- Broecker, W.S., Andree, M., Wolff, W., Oeschger, H., Bonani, G., Kennett, J., Peteet, D., 1988. The chronology of the last deglaciation: Implications to the cause of the Younger Dryas event. *Paleoceanography* 3 (1), 1–19.
- Broecker, W.S., Peteet, D.M., Rind, D., 1985. Does the ocean-atmosphere system have more than one stable mode of operation?. *Nature* 315, 21–26.
- Broström, A., Coe, M., Harrison, S.P., Gallimore, R., Kutzbach, J.E., Foley, J., Prentice, I.C., Behling, P., 1998. Land surface feedbacks and paleomonsoons in northern Africa. *Geophysical Research Letters* 25 (19), 3615–3618.
- Brovkin, V., Claussen, M., Petoukhov, V., Ganopolski, A., 1998. On the stability of the atmosphere-vegetation system in the Sahel/Sahara region. *Journal of Geophysical Research* 103 (D4), 31613–31624.
- Claussen, M., Brovkin, V., Ganopolski, A., Kubatzki, C., & Petoukhov, V. (1998). Modeling global terrestrial vegetation-climate interaction. *Philosophical Transactions of the Royal Society of London*, 353 (B).
- Claussen, M., Kubatzki, C., Brovkin, V., Ganopolski, A., Hoelzmann, P., Pachur, H.-J. (1999). Simulation of an abrupt change in Saharan vegetation in the mid-Holocene. *Geophysical Research Letters*.
- Clemens, S., Prell, W., Murray, D., Shimmield, G., Weedon, G., 1991. Forcing mechanisms of the Indian Ocean monsoon. *Nature* 353, 720–725.
- Clemens, S.C., Prell, W.L., 1990. Late Pleistocene variability of Arabian Sea summer monsoon winds and continental aridity: Eolian records from the lithogenic component of deep-sea sediments. *Paleoceanography* 5, 109–145.
- Coe, M., Bonan, G., 1997. Feedbacks between climate and surface water in northern Africa during the middle Holocene. *Journal of Geophysical Research* 102 (D10), 11087–11101.
- COHMAP Members (1988). Climatic changes of the last 18,000 years: Observations and model simulations. *Science*, 241, 1043–1052.
- Dansgaard, W., et al., 1993. Evidence for general instability of past climate from a 250-kyr ice core record. *Nature* 364, 218–220.
- deMenocal, P.B., Rind, D., 1993. Sensitivity of Asian and African climate to variations in seasonal insolation, glacial ice cover, sea-surface temperature, and Asian orography. *Journal of Geophysical Research* 98 (4), 7265–7287.
- Druyan, L.M., 1987. GCM studies of the African monsoon. *Climatic Dynamics* 2, 117–126.
- Faure, H., Manguin, E., Nydal, R., 1963. Formations lacustres du Quaternaire supérieur du Niger oriental: diatomites et âges absolus. *Bulletin de Bureau de Recherches de Géologie et Minières* 3, 41–63.
- Fischer, G., Donner, B., Ratmeyer, V., Davenport, R., Wefer, G., 1996. Distinct year-to-year particle flux variations off Cap Blanc during 1988–1991: Relation to $\delta^{18}\text{O}$ -deduced sea-surface temperatures and trade winds. *Journal of Marine Research* 54, 73–98.

- Foley, J., Kutzbach, J., Coe, M., Levis, S., 1994. Feedbacks between climate and boreal forests during the Holocene epoch. *Nature* 371, 52–53.
- Foley, J.A., 1994. The sensitivity of the terrestrial biosphere to climatic change: A simulation of the middle Holocene. *Global Biogeochemical Cycles* 8 (4), 505–525.
- Fontaine, B., Bigot, S., 1993. West African rainfall deficits and sea-surface temperatures. *International Journal of Climatology* 13, 271–285.
- Ganopolski, A., Kubatzki, C., Claussen, M., Brovkin, V., Petoukhov, V., 1998. The influence of vegetation-atmosphere-ocean interaction on climate during the mid-Holocene. *Science* 280, 1916–1919.
- Gasse, F., Lédée, V., Massault, M., Fontes, J.C., 1989. Water level fluctuations of Lake Tanganyika in phase with oceanic changes during the last glaciation and deglaciation. *Nature* 342, 57–59.
- Gasse, F., Téhét, R., Durand, A., Gibert, E., Fontes, J.C., 1990. The arid-humid transition in the Sahara and Sahel during the last deglaciation. *Nature* 346, 141–146.
- Gasse, F., Van Campo, E., 1994. Abrupt post-glacial climate events in West Asia and North Africa monsoon domains. *Earth and Planetary Science Letters* 126, 435–456.
- Gasse et al. 1999. Hydrological changes in the African tropics since the Last Glacial Maximum. *Quaternary Science Reviews* 19, this issue.
- Grousset, F.E., Parra, M., Bory, A., Martinez, P., Bertrand, P., Shimmiel, G., Ellam, R.M., 1998. Saharan wind regimes traced by the Sr-Nd isotopic composition of subtropical Atlantic sediments: last glacial maximum vs. today. *Quaternary Science Reviews* 17, 395–409.
- Henning, D., Flohn, H., 1981. Some aspects of evaporation and sensible heat flux of the tropical Atlantic. *Contributions to Atmospheric Physics* 53 (3), 430–441.
- Hewitt, C.D., Mitchell, J.F.B.H., 1998. A fully coupled GCM simulation of the climate of the mid-Holocene. *Geophysical Research Letters* 25 (3), 361–364.
- Hoelzmann, P., Jolly, D., Harrison, S.P., Laarif, F., Bonnefille, R., Pachur, H.-J., 1998. Mid-Holocene land surface conditions in northern Africa and the Arabian Peninsula: A data set for the analysis of biogeochemical feedbacks in the climate system. *Global Biogeochemical Cycles* 12, 35–52.
- Jäkel, D., 1979. Run-off and fluvial formation processes in the Tibesti Mountains as indicators of climatic history in the central Sahara during the late Pleistocene. *Palaeoecologia Africana* 11, 13–44.
- Johnson, T.C., Scholz, C.A., Talbot, M.R., Kelts, K., Ricketts, R.D., Ngobi, G., Beuning, K., Ssemmanda, I., McGill, J.W., 1996. Late Pleistocene desiccation of Lake Victoria and rapid evolution of cichlid fishes. *Science* 273, 1091–1093.
- Jolly, D., et al., 1998. Biome reconstruction from pollen and plant macrofossil data for Africa and the Arabian Peninsula at 0 and 6 ka. *Journal of Biogeography* 25, 1007–10027.
- Knaack, J.J., 1997. Eine neue Transferfunktion zur Rekonstruktion der Paläoproduktivität aus Gemeinschaften mariner Diatomeen. *Berichte-Reports, Geol.-Paläont. Inst. Univ. Kiel* 83, 1–118.
- Kohfeld and Harrison, 1999. How well can we simulate past climates? Evaluating the models using global palaeoenvironmental data sets. *Quaternary Science Reviews*, 19 this issue.
- Kolla, V., Biscaye, P.E., Hanley, A.F., 1979. Distribution of quartz in late Quaternary Atlantic sediments in relation to climate. *Quaternary Research* 11, 261–277.
- Kutzbach, J.E., 1996. Vegetation and soil feedbacks on the response of the African monsoon to orbital forcing in the early to middle Holocene. *Nature* 384, 623–626.
- Kutzbach, J.E., Guetter, P.J., 1986. The influence of changing orbital parameters and surface boundary conditions on climate simulations for the past 18,000 year. *Journal of Atmospheric Science* 43, 1726–1759.
- Kutzbach, J.E., Liu, Z., 1997. Response of the African monsoon to orbital forcing and ocean feedbacks in the middle Holocene. *Science* 278, 440–444.
- Kutzbach, J.E., Otto-Bliesner, B.L., 1982. The sensitivity of the African-Asian monsoonal climate to orbital parameter changes for 9000 years BP in a low-resolution general circulation model. *Journal of Atmospheric Science* 39, 1177–1188.
- Lamb, H.F., Gasse, F., Benkaddour, A., El Hamouti, N., van der Kaars, S., Perkins, W.T., Pearce, N.J., Roberts, C.N., 1995. Relation between century-scale Holocene arid intervals in tropical and temperate zones. *Nature* 373, 134–137.
- Lezine, A.M., 1991. West African paleoclimates during the last climatic cycle inferred from an Atlantic deep-sea pollen record. *Quaternary Research* 35, 456–463.
- Lezine, A.-M., Casanova, J., Hillaire-Marcel, C., 1990. Across an early Holocene humid phase in western Sahara: Pollen and isotope stratigraphy. *Geology* 18, 264–267.
- Manabe, S., Stouffer, R.J., 1988. Two Stable Equilibria of a Coupled Ocean-Atmosphere Model. *Journal of Climate* 1, 841–866.
- Manabe, S., Stouffer, R.J., 1995. Simulation of an abrupt climate change induced by freshwater input to the North Atlantic Ocean. *Nature* 378, 165–167.
- Mangerud, J., 1987. The Allerød/Younger Dryas boundary. In: Berger, W.H., Labeyrie, L.D. (Eds.), *Abrupt Climatic Change*. D. Reidel Publishing Company, Dordrecht, pp. 163–171.
- Masson, V., Joussaume, S., 1997. Energetics of the 6000-yr BP atmospheric circulation in Boreal summer, from large-scale to monsoon areas: A study with two versions of the LMD AGCM. *Journal of Climate* 10, 2888–2902.
- McIntosh, S.K., McIntosh, R.J., 1983. Current directions in West African prehistory. *Annual Review of Anthropology* 12, 215–258.
- McIntyre, A., Ruddiman, W.F., Karlin, K., Mix, A.C., 1989. Surface water response of the equatorial Atlantic Ocean to orbital forcing. *Paleoceanography* 4 (1), 19–55.
- Middleton, N., 1987. Desertification and wind erosion in the western Sahel: the example of Mauritania. *School of Geography. University of Oxford, Research Paper* 40, 1–26.
- Molano, B., McIntyre, A., 1990b. Precessional forcing of nutricline dynamics in the equatorial Atlantic. *Science* 249, 766–769.
- Mortlock, R.A., Froelich, P.N., 1989. A simple method for the rapid determination of biogenic opal in pelagic marine sediments. *Deep-Sea Research* 36, 1415–1426.
- Moulin, C., Lambert, C., Dulac, F., Dayan, U., 1997. Control of atmospheric export of dust from North Africa by the North Atlantic oscillation. *Nature* 387, 691–694.
- Munson, P.J., 1981. A late Holocene (c. 4500–2300) climatic chronology for the southwest Sahara. *Palaeoecologia Africana* 13, 53–60.
- Oeschger, H., Welten, M., Eicher, U., Moll, M., Riesen, T., Siegenthaler, U., Wegmüller, S., 1980. 14C and other parameters during the Younger Dryas cold phase. *Radiocarbon* 22 (2), 299–310.
- Pachur, H.-J., Altman, N. (1997). The Quaternary (Holocene, ca. 8000a BP). In H. Schandelmeyer, & Reynolds, P.-O. *Paleogeographic-paleotectonic atlas of northeastern Africa, Arabia, and adjacent areas Late Neo-Proterozoic to Holocene*. Rotterdam: Balkema.
- Papenfuss, T., 1999. Glazial-interglaziale Variation von Planktonproduktivität und Nährstoffgehalten im tropisch-subtropischen Ostatlantik im Abbild der Barium-Gehalte. *Berichte-Reports, Inst. fuer Geowissenschaften, Univ. Kiel* 5, 1–119.
- Petit-Maire, N., Guo, Z., 1996. Mis en evidence de variations climatiques Holocenes rapides, en phase dans les deserts actuels de Chine et de Nord de l'Afrique. *Sciences de la Terre et des Planetes* 322, 847–851.
- Petit-Maire, N., Fabre, J., Carbonel, P., Schulz, E., Aucour, A.M., 1987. La depression de Taoudeni (Sahara malien) a l'Holocene. *Geodynamique* 2, 61–67.
- Pokras, E.M., Mix, A.C., 1987. Earth's precession cycle and Quaternary climatic change in tropical Africa. *Nature* 326, 486–487.
- Prell, W.L., Kutzbach, J.E., 1987. Monsoon variability over the past 150,000 years. *Journal of Geophysical Research* 92, 8411–8425.

- Prospero, J., 1981. Arid regions as sources of mineral aerosols in the marine atmosphere. *Geological Society of America Special Publications* 186, 71–86.
- Prospero, J.M., Nees, R.T., 1977. Dust concentration in the atmosphere of the equatorial North Atlantic; possible relationship to Sahelian drought. *Science* 196, 1196–1198.
- Prospero, J.M., Nees, R.T., 1986. Impact of North African drought and el Nino on mineral dust in the Barbados trade winds. *Nature* 320, 735–738.
- Pye, A.C., 1987. In: *Eolian Dust and Dust Deposits*. Academic Press, New York.
- Rahmstorf, S., 1995. Bifurcations of the Atlantic thermohaline circulation in response to changes in the hydrological cycle. *Nature* 378, 145–150.
- Ritchie, J.C., Eyles, C.H., Haynes, C.V., 1985. Sediment and pollen evidence for an early to mid-Holocene humid period in the eastern Sahara. *Nature* 330, 645–647.
- Roberts, N., 1998. In: *The Holocene* Oxford, Blackwell, 316 pp.
- Roberts, N., Lamb, H.F., El Hamouti, N., Barker, P., 1994. Abrupt Holocene hydroclimatic events: Palaeolimnological evidence from Northwest Africa. In: Pye, A.C.M.a.K. (Ed.), *Environmental Change in Drylands: Biogeographical and Geomorphological Perspectives*. Wiley, London, pp. 163–175.
- Roberts, N., Taieb, M., Barker, P., Danati, B., Icole, M., Williamson, D., 1993. Timing of the Younger Dryas event in East Africa from lake-level changes. *Nature* 366, 146–148.
- Rognon, P., 1983. Essai de definition et typologie des crises climatiques. *Bull. Inst. Geol. Bassin Aquitaine* 34, 151–164.
- Rosignol-Strick, M., 1985. Mediterranean quaternary sapropels, an immediate response of the African Monsoon to variation of insolation. *Palaeogeography, palaeoclimatology, palaeoecology* 49, 237–263.
- Ruddiman, W., Sarnthein, M., Baldauf, J., 1988. Proceedings of the Ocean Drilling Program Leg 108, U. S. G. P. Off., Ed., pp. 1073.
- Sarnthein, M., 1978. Sand deserts during the glacial maximum and climate optimum. *Nature*, 272, 43–46.
- Sarnthein, M., Erlenkeuser, H., Zahn, R., 1982. Termination I: The response of continental climate in the subtropics as recorded in deep-sea sediments. *Bull. Inst. du Bassin d'Aquitaine* 31, 393–407.
- Sarnthein, M., Tiedemann, R., 1989. Toward a high-resolution stable isotope stratigraphy of the last 3.4 million years: Sites 658 and 659 off northwest Africa. In: Ruddiman, W., Sarnthein, M. (Eds.), *Proceedings of the ocean drilling program, scientific results, Ocean Drilling Program*. College Station, TX, pp. 167–185.
- Schütz, L., Jaenicke, R., Pietrek, H., 1981. Saharan dust transport of the North Atlantic Ocean. *Geological Society of America Bulletin Special Paper* 186, 87–100.
- Sowers, T., Bender, M., 1995. Climate records covering the last deglaciation. *Science* 269, 210–214.
- Stocker, T.F., Wright, D.G., Broecker, W.S., 1992. The influence of high-latitude surface forcing on the global thermohaline circulation. *Paleoceanography* 7, 529–541.
- Street, F.A., Grove, A.T., 1979. Global maps of lake-level fluctuations since 30,000 years BO. *Quaternary Research* 12, 83–118.
- Street-Perrott, F.A., Mitchell, J.F.B., Marchand, D.S., Brunner, J.S., 1990. Malankovitch and albedo forcing of the tropical monsoon: A comparison of geological evidence and numerical simulations for 9000 yr BP. *Transactions of the Royal Society of Edinburgh (Earth Science)* 81, 407–427.
- Street-Perrott, F.A., Harrison, S.A., 1984. Temporal variations in lake levels since 30,000 yr BP – An index of the global hydrological cycle. In: Hansen, J.E., Takahashi, T. (Eds.), *Climate Processes and Climate Sensitivity*. Amer. Geophys. Union, Wash. DC, pp. 118–129.
- Street-Perrott, F.A., Perrott, R.A., 1990. Abrupt climate fluctuations in the tropics: the influence of Atlantic Ocean circulation. *Nature* 343, 607–612.
- Stuiver, M., Reimer, P.J., 1993. Extended 14C data base and revised CALIB 3.0 14C age calibration program. *Radiocarbon* 35, 215–230.
- Talbot, M.A., Delbrias, G., 1980. A new late Pleistocene-Holocene water level curve for Lake Bosumtwi, Ghana. *Earth Planetary Science Letters* 47, 336–344.
- Talbot, M.R., 1980. Environmental responses to climatic change in the West African Sahel over the past 20,000 years. In: Williams, M.A., Faure, H. (Eds.), *The Sahara and the Nile*. Balkema, Rotterdam, pp. 527–582.
- Tetzlaff, G., Wolter, K., 1980. Meteorological patterns and the transport of mineral dust from the North African continent. *Paleoecol. Africa* 12, 31–42.
- Tiedemann, R., Sarnthein, M., Shackleton, N.J., 1994. Astronomic time-scale for the Pliocene Atlantic $\delta^{18}\text{O}$ and dust flux records of ODP Site 659. *Paleoceanography* 9 (4), 619–638.
- Webster, P.J., 1987. The variable and interactive monsoon. In: Fein, J.S., Stephens, P.L. (Eds.), *Monsoons*. Wiley, New York, pp. 269–330.
- Williamson, D., Taieb, M., Damnati, B., Icole, M., Thouveny, N., 1993. Equatorial extension of the Younger Dryas event: rock magnetic evidence from Lake Magadi (Kenya). *Global and Planetary Change* 7, 235–242.